



## Supporting Online Material for

### **Climate-Driven Ecosystem Succession in the Sahara: The Last 6000 Years**

S. Kröpelin,\* D. Verschuren, A.-M. Lézine, H. Eggermont, C. Cocquyt, P. Francus,  
J.-P. Cazet, M. Fagot, B. Rumes, J. M. Russell, F. Darius, D. J. Conley,  
M. Schuster, H. von Suchodoletz, D. R. Engstrom

\*To whom correspondence should be addressed. E-mail: s.kroe@uni-koeln.de

Published 9 May 2008, *Science* **320**, 765 (2008)  
DOI: 10.1126/science.1154913

#### **This PDF file includes:**

Materials and Methods  
SOM Text  
Figs. S1 to S4  
Tables S1 and S2  
References

## Materials and Methods

1. Lake Yoa almost certainly contains a complete sequence of Holocene environmental change (*S1*); only the mid- and late-Holocene portion could be recovered with light-weight coring equipment (*S2*) operated with casing in 24.3 m water depth. The sampled sediments (composite core OUNIK03/04; 7.47 m long) are finely laminated clayey to sandy muds with 5-20% organic matter, 5-25% carbonate, and 1-13% diatom silica. In the lower half of the core (7.47-4.25 m), lamination couplets are composed of a dark brown to black organic lamina and a white lamina of endogenic calcite, occasionally supplemented by a thin red-brown lamina of wind-blown silt (Fig. 2D). In the upper half of the core (4.25-0.00 m) the red-brown laminae are thicker (4-18 mm), more frequent, and grade into the organic laminae. Above 1.57 m, almost all carbonate is detrital, and embedded within the red-brown laminae.

2. Sediment chronology was established using the  $^{137}\text{Cs}$ -inferred time marker of nuclear bomb testing in 1963-1964 (*S3*), and 17 accelerator mass spectrometry (AMS)  $^{14}\text{C}$  dates on charred grass, fragments of *Typha* rhizome, or bulk organic matter. A count of 39 lamination couplets above the AD 1964  $\pm$  3 yr  $^{137}\text{Cs}$  peak supports their classification as varves. Paired  $^{14}\text{C}$  dates on *Typha* rhizomes and bulk organic matter yield similar results (Table S1), indicating that most carbon uptake in the root system of these stands is from the water. Our calendar age-depth model (Fig. S1) is a 3<sup>rd</sup>-order polynomial regression of INTCAL04-calibrated  $^{14}\text{C}$  ages (*S4*) vs. cumulative dry weight down-core, after removal of three outliers and subtraction of the modern lake-carbon reservoir age from all bulk organic and *Typha* rhizome ages. This modern lake-carbon reservoir correction ( $1467 \pm 44$   $^{14}\text{C}$  years) is the mean  $^{14}\text{C}$  age difference ( $n = 3$ ) between two pairs of  $^{14}\text{C}$  dates on terrestrial and aquatic organic matter, and between the uppermost  $^{14}\text{C}$  date on bulk organic matter and its corresponding varve count (Table S1). Given dating uncertainty resulting from analytical and age-modeling error (mean  $\pm$  40  $^{14}\text{C}$  years and  $\pm$  70 calendar years, respectively), all calendar ages given in the text are rounded to the nearest 100 years. Preliminary varve counts on the whole sequence duplicate the  $^{14}\text{C}$  chronology within the error range of both techniques.

3. Fossil diatom sample processing followed refs. *S5-S6*. Changes through time in the fossil diatom assemblage were identified using stratigraphically constrained sum-of-squares cluster analysis (CONISS; *S7*) applied to squared-root transformed species percentage data. The statistical significance of this zonation was assessed following refs. *S8-S9*, using ZONE 1.2 (*S10*) and BSTICK 1.0 (*S11*). Biostratigraphic diagrams were produced in TILIA 2.0.b.4. (*S12*) and TGView 2.0.2 (*S13*). Reconstructed paleosalinity (as conductivity, in  $\mu\text{S}/\text{cm}$ ) is the weighted mean value of 5 lakes with modern diatom species composition most similar to the fossil Lake Yoa assemblage (weighted modern-analogue technique, WMAT). We used a calibration dataset containing 264 samples from  $\sim$ 150 African waters (*S14*) supplemented by 20 samples from 9 waters in the Ounianga region. This transfer function has an  $r^2_{\text{jack}}$  between inferred and observed log-transformed conductivity of 0.76, and a root-mean-square error of prediction (RMSEP) of 0.44  $\log_{10}$  conductivity units. All 94 fossil assemblages found good modern analogues (*S15*) in the calibration data set. Sample-specific errors (*S16*) range from 0.48-0.59  $\log_{10}$  conductivity units in the freshwater lake phase to 0.46-0.66  $\log_{10}$  conductivity units in the hypersaline lake

phase (Fig. 2A). Salinity inferences, analogue statistics and sample-specific errors were obtained in C2 1.3.4. (S17).

4. Aquatic invertebrate fauna analysed include the Chironomidae, Chaoboridae and Ephydriidae (all Insecta Diptera), Corixidae (Insecta Hemiptera), and Chydoridae (Crustacea Anomopoda). Chaoboridae (phantom midges) and Corixidae (waterboatmen) are planktonic organisms. Ephydriidae (brine flies) are in Lake Yoa restricted to sandy shoreline habitat. Chironomidae (non-biting midges) and Chydoridae (water fleas *partim*) are benthic, and in this stratified lake restricted to oxygenated shallow-water bottom habitat. Given the stable sedimentation dynamics, taphonomy and preservation of these chitinous invertebrate remains can be assumed constant throughout the studied sequence. Sample processing followed refs. S18-S19. Identification was done at 100 to 400-fold magnification using guides for sub-Saharan Africa (S20-S24). Counting criteria for fragmentary fossils followed ref. S18, and sample volumes were adjusted to yield the diversity-dependent fossil sum required for robust numerical analysis (S25-S26). Chironomid-based salinity inference is based on WMAT applied to an African calibration dataset of chironomid community composition in 87 lakes (72 in East Africa, 8 in West Africa, 7 from within the Sahara; S27). This transfer function has an  $r^2_{\text{jack}}$  between inferred and observed log-transformed conductivity of 0.77, and a RMSEP of 0.40  $\log_{10}$  conductivity units. On average 96 % of the fossil chironomid sum in individual samples were taxa represented in the calibration dataset; the remainder (e.g., *Chironomus* indet. sp.) are almost certainly Eurasian chironomid species with undocumented salinity tolerance (S27). Excluding these taxa, all 93 fossil assemblages found good modern analogues (S15) in the calibration data set. Sample-specific errors (S16) range from 0.48-0.66  $\log_{10}$  conductivity units in the freshwater lake phase to 0.42-0.48  $\log_{10}$  conductivity units in the hypersaline lake phase.

5. Pollen samples were processed according to standard procedures (S28) including treatment with HCL and HF, and sieving through 5  $\mu\text{m}$  mesh. Addition of a known amount of exotic pollen (*Alnus*) allowed calculation of pollen concentrations (grains per ml) and fluxes (grains per  $\text{cm}^2$  per year). In total 163 different pollen types were identified for a mean pollen sum of 406 (range 88-848) counted plant pollen and fern spores per sample. The recovered plant taxa represent the modern Mediterranean, Saharan, Sahelian, Sudanian and Tibesti-montane phytogeographical zones. Mediterranean plant taxa in Fig. 2 are mainly *Olea*, *Quercus* and *Pistacia*; Saharan plant taxa are mainly the trees *Salvadora persica* and *Ephedra*, and herbs *Artemisia*, *Cornulaca* and Amaranthaceae-Chenopodiaceae; tropical (Sudanian) plant taxa are mainly the trees *Piliostigma*, *Lannea* and *Fluggea virosa*, and herbs *Mitracarpus* and *Spermacoce*. Pollen slides also contained diagnostic remains of phytoplankton species. These could be attributed to 23 taxa of Chlorophyta (green algae), 2 taxa of Cyanobacteria (blue-green algae), and 1 taxon of Dinophyta (dinoflagellates); see Table S2.

6. Low-field magnetic susceptibility was measured on a Geotek multisensor core logger at 1 cm resolution, using a Bartington MS2E point sensor. Data are presented as mass-specific magnetic susceptibility ( $\chi$ ) with organic and carbonate content subtracted from total dry mass. Magnetic susceptibility measures the concentration of magnetic particles in sediments, proportional to total allochthonous mineral matter in lakes and to the relative concentration of different magnetic minerals present in the source deposit of this allochthonous matter (S29). Which iron-bearing mineral is primarily responsible for the magnetic properties of the sediment depends on the history of weathering regimes in the source region. In lake Yoa today, allochthonous mineral

matter is mainly the wind-blown silt that accumulates in the thin red-brown lamina, and is enriched in Fe-rich minerals. The warm and dry climate conditions which during the late Quaternary most commonly prevailed in its source region (the Ounianga area and southern Libya to the northeast) favour the formation of hematite through secondary alteration of goethite present in soils and iron crusts (*S30-31*).

## Supporting online text

**1. *Lack of continuous records of Saharan climate and ecosystem change.*** The now numerous available Holocene paleolake records from the arid and subarid belts of North Africa (for a recent synthesis see ref. *S32*) document a fairly consistent scheme of an early-Holocene moist and green Sahara followed by general aridification, but pronounced differences in the apparent timing and amplitude of hydrological change inferred from individual records point to both regional variability in climate change and site-specific topographic or hydrogeological influences on reconstructed water-balance evolution (*S33-S34*). In addition the ubiquitous temporal hiatuses in Saharan lake-sediment archives due to desiccation, and any changes in sediment accumulation that are inadequately constrained chronologically, cryptically over-accentuate directional trends in the paleohydrological proxies (*S35*), thereby compromising inferences of the rates of climate or ecosystem change. Consequently, inferences of abrupt mid-Holocene drying (e.g., *S36*) or of fluctuations between moist and dry episodes (e.g., *S37-S38*) based on such individual records are difficult to substantiate, and analysis of possible regional synchrony of climate events is problematic (*S33*). At the same time, poor age control on individual records and the site-specific relationship between local water balance and climate cause supra-regional summaries of Saharan lake status through time (*S39*) to suggest more gradual climate change than may actually have occurred, besides obscuring the well-established north-south gradient in the timing of Holocene aridification over North Africa (*S34, S40*). These problems explain the attractiveness of a proxy record of Saharan climate and ecosystem change extracted from marine sediments (*S41*), a paleoenvironmental archive that is generally trusted to accumulate continuously and to faithfully monitor an areally integrated rate of change in the moisture balance on nearby continents. However, also in this record the inferred rate of terrestrial ecosystem change is affected by major variation in sediment accumulation (*S42*). Further, there is continued uncertainty about the size and location of the Saharan source region (formerly) supplying dust to that particular area of the tropical Atlantic Ocean (*S43*). Thus, only a demonstrably continuous and adequately-dated paleoenvironmental record from within the desert, such as the Lake Yoa record presented here, can reveal the true rate and trajectory of terrestrial ecosystem change associated with the Holocene desiccation of the Sahara.

**2. *Modern climatology and vegetation of the Ounianga region.*** Monthly mean day- and nighttime temperatures at Ounianga Kebir vary 26-42 °C and 15-26 °C during the year. Annual rainfall is erratic, ranging 0-21 mm between 1953 and 1967 (mean 3.9 mm; n = 15). Summer monsoon rainfall from the south does not occur regularly within ~300 km of the area, and wintertime depressions from the Mediterranean only occasionally reach the Tibesti, 400 km to the northwest. Monthly pan evaporation was measured at Faya Largeau (200 km to the southwest) from 1987 to 2002 (n = 16) but many values are missing. Mean annual evaporation derived from three complete annual data sets (1989, 1993, 1999) is 6330 mm; the sum of mean values available for each month (n = 9-14) is 6110 mm (weather data courtesy of the Direction des Ressources en Eau et de la Météorologie, N'Djamena, Chad). Vegetation surrounding Lake Yoa is of desert type, with plants confined to dry river beds (*S44*) except date palm (*Phoenix*), cattail (*Typha*) and some *Acacia* growing near the lakeshore.

**3. *Ecological succession in the Lake Yoa phytoplankton community.*** Before 5600 cal yr BP the algal flora was characterized by the green algae *Botryococcus*, *Spirogyra* and Hydrodyctiaceae

(Fig. S2) and the diatoms *Aulacoseira*, *Chaetoceros* and *Urosolenia* (Fig. S3). After that time *Aulacoseira* and *Synedra* became the most prominent diatoms (Fig. S3); among green algae, *Botryococcus* and *Spirogyra* were replaced by Desmidiaceae (*Cosmarium*, *Staurastrum*) and Scenedesmaceae (*Scenedesmus*, *Coelastrum*), which reached peak abundances ~5500-5200 cal yr BP. These and other green algae almost disappeared ~4900-4800 cal yr BP, when diatom production (% biogenic SiO<sub>2</sub>; Fig. 2B) again increased together with a slight rise in diatom-inferred lake-water salinity from 300 μS/cm to ~600 μS/cm (Fig. 2A). Inference of rising salinity reflects the appearance of salt-tolerant diatoms (*Nitzschia fonticola*, *N. cf. elliptica*, *Rhopalodia gibberula*, *Stauroneis*) at the expense of *Aulacoseira* (Fig. S3). The transition of Lake Yoa from a fresh to salt-lake environment between 4200 and 3900 cal yr BP is marked in the fossil diatom record by complete collapse of the formerly dominant *Aulacoseira* population. This benefited the salt-tolerant species already present, and newly appearing salt-loving taxa (Fig. S3: *Anomoeoneis sphaerophora*, *Nitzschia frustulum*). Paleoecological interpretation and salinity inference based on the fossil diatom record after 3900 cal yr BP is complicated by the presence of taxa with unknown ecological affinity, and by contamination of the local salt-lake species assemblages with freshwater taxa eroded from early-Holocene diatomites exposed nearby. Incongruent freshwater diatom assemblages containing *Aulacoseira*, *Synedra* and *Campylodiscus* continue to be deposited in Lake Yoa today, and even dominate the fossil record since 2700 cal yr BP because autochthonous diatom production in this hypersaline environment has been virtually non-existent (Fig. 2B: ~3% biogenic SiO<sub>2</sub>; Fig. S2: on average 0.13×10<sup>6</sup> diatom frustules per mg dry sediment). After correcting for these known complicating factors, the diatom-inferred conductivity for Lake Yoa has a rather stable mean value of ~10,000 μS/cm for the past ~3600 years, still significantly below the observed modern value of 69,000 μS/cm. We attribute this difference mainly to the lack of hypersaline calibration lakes with diatom flora similar to that of the modern Lake Yoa.

**4. Ecological succession in the Lake Yoa zooplankton and zoobenthos.** The stratigraphic distribution of aquatic insects and microcrustaceans (Figs. S2, S4) confirms that until 4800 cal yr BP Lake Yoa was a deep and dilute freshwater environment with diverse nearshore habitat including submerged vegetation. Impact of evaporative concentration on the osmotic balance of these aquatic plants is indicated from 4800 cal yr BP by reduction in *Polypedilum* nr. *deletum* and vegetation-dwelling Chydoridae (S45). Secondary productivity of Lake Yoa (as indicated by fossil chironomid abundance; Fig. S4) peaked during the fresh-to-saline transition at 4200-3900 cal yr BP. It started to decrease when conductivity rose above the critical physiological threshold of 3000 μS/cm (S46-S47), and virtually all salt-intolerant freshwater zoobenthos were eradicated. In the meso- to hypersaline environment prevailing after that time, secondary productivity stabilised at ~30% of the mean value attained during the freshwater phase. The transition to a true salt-lake community at 3400 cal yr BP is indicated by the disappearance of all remaining Chydoridae, *Chaoborus*, and freshwater Chironomidae (*Dicrotendipes* cf. *kribiicola*, *Cladotanytarsus pseudomancus*).

**5. Quality of the Lake Yoa record as paleoenvironmental archive.** The continuously laminated deposits recovered from Lake Yoa testify that, notwithstanding its evolution from a fresh to hypersaline ecosystem, the water-column and sedimentation processes which control its incorporation of climate proxies and ecological indicators in the sediment record have remained constant throughout the last 6000 years. Furthermore the almost linear age-depth relationship ( $r^2$  of age versus depth = 0.982;  $r^2$  of age versus cumulative dry weight = 0.985; n = 14) indicates

that the rate of profundal sediment accumulation has been near-constant through time. Therefore, absolute concentrations of sediment components (organic matter, biogenic SiO<sub>2</sub>, sand) and the fossils contained in them approximate their true rate (flux) of offshore deposition through time. For example, since organic matter preservation and its dilution by mineral sediments has remained more or less unchanged, the principal trends in % organic matter through time can be treated as reflecting change in aquatic primary production.

**6. Proxy indicators of wind strength.** We hypothesize that in the currently hypersaline lake, dune sand is transported to the mid-lake coring site mostly by saltation from a nearby dune into the lake followed by entrapment in a soapy film at the water surface. Thus, sand content of offshore sediments is primarily a function of dune size and proximity. For example, coincidence of a reduction in *Typha* pollen since ~1700 cal yr BP with sand values rising to > 20% of the dry sediment indicate that expanding dunes encroached upon suitable *Typha* habitat along Lake Yoa's northern shore (cf. Fig. 1C). Background values of 1-5% fine sand in the lower part of the record can be attributed to surface runoff and/or river input from a vegetated landscape. Availability of larger quantities of sand to start building lakeshore dunes from 3700 cal yr BP evidently also reflects the increasing mobilization of sand following regional loss of vegetation cover, but the direct relationship of profundal sand content with climatic drought or wind strength is unclear. In contrast, total fine-grained aeolian input (reflected in sediment magnetic susceptibility; see *S31*) is proportional to the fraction of the landscape lacking vegetation cover, as long as the supply of loose soil weathered during previous wetter periods is unlimited. Our combined evidence indicates that in northern Chad this was the case between 4300 and 2700 cal yr BP. Stable background values of magnetic susceptibility before 4300 cal yr BP are consistent with palynological evidence that regional vegetation cover (mostly grassland) was close to 100%. The spike in magnetic susceptibility at ~4200 cal yr BP may indicate that the earliest vegetation loss was relatively abrupt, or alternatively that early dust storms were infrequent high-volume events. After 2700 cal yr BP, mineral dust flux became limited by the rate of new erosion of suitable sediments and rocks in the now mostly barren landscape. Total pollen influx (and after 4000 cal yr BP grass pollen influx) is mainly a function of wind strength and remaining grass cover. Trade-wind direction in the region has not changed since the early Holocene (*S48-S49*), due to topographic control of the Tibesti-Ennedi corridor.

**7. Incongruent occurrence of pollen taxa.** Scattered occurrences of tropical pollen types in the upper part of the sequence (after 2700 cal yr BP) were probably eroded from early-Holocene lake deposits nearby. An olive species endemic to the Saharan mountains, *Olea laperrini*, dominated mid-Holocene vegetation at ~2150 m in the Ahaggar massive (*S50*). Given its complete absence in the contemporaneous core interval at Lake Yoa, this species is unlikely to be the source of *Olea* pollen deposited in Lake Yoa after 2500 cal yr BP.

**8. Evidence for mid-Holocene climatic fluctuations.** Some vegetation (*S37*) and hydrological (*S38*, *S51-S52*) records as well as regional compilations of <sup>14</sup>C dates on lacustrine deposits (*S53*) suggest that the mid-Holocene drying of the Sahara proceeded as a series of multi-decadal or century-scale fluctuations between moist and dry episodes superimposed on the long-term drying trend. Such rapid climate and ecosystem swings are also produced by model simulations incorporating decade-scale climate variability (*S39*, *S54-S55*). The Lake Yoa record shows marked cyclic variation in pollen influx at ~600-year intervals between 6000 and 4300 cal yr BP (Fig. 2G), with the timing of influx minima (at 5800-5600 and 5100-4800 cal yr BP) broadly

matching the timing of drought spells inferred from a tree-ring record in southwestern Libya (S52). However, influx rates of all major terrestrial pollen types (grasses, *Acacia*, tropical plant taxa, *Erica* type *arborea*) are affected in near-equal fashion, and pollen percentage data (e.g., % grasses: Fig. 2G) show a gradual decline throughout this period. We therefore ascribe the century-scale pollen influx fluctuations to variation in the proportion of air- and river-borne pollen input to Lake Yoa, rather than to real shifts in the regional vegetation ecotone. Thus, pollen influx maxima at 6100-5900, 5500-5200, and 4900-4700 cal yr BP represent climatically wet episodes when enhanced discharge of a possibly seasonal river (wadi) into Lake Yoa brought a greater proportion of pollen types from higher (and naturally wetter) areas on the eastern slopes of the Tibesti. We envision that such century-scale rainfall fluctuations between 6000 and 4300 cal yr BP had sufficient amplitude to affect highland tree growth (S52) and elicit a marked hydrological response in some Saharan lakes that were isolated from the regional groundwater table, but not in the groundwater-buffered Lake Yoa. More importantly, these rainfall fluctuations did not measurably interrupt the gradual southward retreat of vegetation ecotones during the mid-Holocene. In the aquatic ecosystem indicators, we observe 1) a diatom-inferred temporary decrease of Lake Yoa conductivity to  $\sim 4000$   $\mu\text{S}/\text{cm}$  around 2300 cal yr BP after having attained  $>10,000$   $\mu\text{S}/\text{cm}$  in the period 3800-2600 cal yr BP; and 2) a chironomid-inferred decrease to  $\sim 20,000$   $\mu\text{S}/\text{cm}$  in much of the period 2100-1200 cal yr BP, from values  $>25,000$   $\mu\text{S}/\text{cm}$  in the period 3400-2400 cal yr BP. Since both of these inferred salinity reversals depend on abundance changes in just one or a few species of aquatic biota, remain within method- and sample-specific uncertainty ranges, and are not reproduced in other hydrological indicators, we consider the evidence for significant fluctuations in lake water balance during those late-Holocene episodes to be weak.

**9. Inferences of total annual rainfall.** Our data are qualitatively consistent with the gradual decrease from 6000 cal yr BP of monsoon precipitation in the sector  $18\text{-}23^\circ\text{N}$  /  $11\text{-}34^\circ\text{E}$  (which includes the Ounianga region) that is simulated in a synchronously coupled ocean-atmosphere-terrestrial ecosystem GCM (S39). Quantitatively our pollen data indicate a slightly lower annual total of  $\sim 250$  mm at 6000 cal yr BP (allowing tropical savannah with 10-15% tree cover; S56) than the 400 mm simulated in ref. S39, and values of  $< 150$  mm by 4300 cal yr BP and  $< 50$  mm by 2700 cal yr BP. Total annual precipitation required to support savanna vegetation at  $20^\circ$  N latitude is estimated to lie between 180 and 260 mm (S57-S59). However, ecohydrological modeling indicates that the intermittent rainfall regime and large inter-annual climate variability typical of desert fringe ecosystems may allow vegetation persistence at significantly lower values of total annual rainfall (S60). Integration of archaeological, geological, archaeozoological and archaeobotanical data across the eastern Sahara (S40) inferred annual rainfall in the Ounianga region to have fallen to below 150 mm by 3500 cal yr BP.

## Supplementary tables

**Table S1.** Radiometric ( $^{137}\text{Cs}$ ,  $^{14}\text{C}$ ) dates obtained on Lake Yoa composite core OUNIK03/04.

| Comp. Depth<br>cm blf | Cumul. Dry Wt<br>g/cm <sup>2</sup> | Dated Material         | Lab No.   | $^{14}\text{C}$ Age<br>years BP | Error<br>+/- SD | Corr. $^{14}\text{C}$ Age<br>years BP | Cal yr BP   | 2 $\sigma$ range |
|-----------------------|------------------------------------|------------------------|-----------|---------------------------------|-----------------|---------------------------------------|-------------|------------------|
| 7.0                   | 3.820                              | $^{137}\text{Cs}$ peak | SMM       |                                 |                 |                                       | AD 1963     |                  |
| 16.0                  | 8.145                              | varve count            |           |                                 |                 |                                       | AD 1918     |                  |
| 16.0                  | 8.145                              | <i>Typha</i> rhizome   | Poz-8729  | 1380                            | 30              | -80                                   |             |                  |
| 35.0                  | 19.175                             | bulk organic matter    | Poz-8739  | <i>2160</i>                     | 35              | <i>693</i>                            | <i>640</i>  | <i>553-726</i>   |
| 35.0                  | 19.175                             | <i>Typha</i> rhizome   | Poz-8730  | 1900                            | 50              | 433                                   | 430         | 310-550          |
| 36.0                  | 19.797                             | grass charcoal         | Poz-8731  | 315                             | 30              | 315                                   | 384         | 304-464          |
| 59.0                  | 34.091                             | <i>Typha</i> rhizome   | Poz-8733  | 1675                            | 30              | 208                                   | 210         | 0-421            |
| 75.0                  | 43.577                             | <i>Typha</i> rhizome   | Poz-8734  | 2200                            | 100             | 733                                   | 718         | 544-891          |
| 79.0                  | 45.949                             | bulk organic matter    | Poz-8738  | <i>2905</i>                     | <i>30</i>       | <i>1438</i>                           | <i>1389</i> | <i>1272-1506</i> |
| 79.0                  | 45.949                             | <i>Typha</i> rhizome   | Poz-8735  | 2020                            | 40              | 553                                   | 581         | 509-653          |
| 87.0                  | 51.011                             | grass charcoal         | Poz-8736  | 670                             | 30              | 670                                   | 618         | 560-675          |
| 89.0                  | 52.339                             | bulk organic matter    | Poz-5065  | 2225                            | 30              | 758                                   | 676         | 567-786          |
| 118.5                 | 68.782                             | bulk organic matter    | Poz-5122  | 1930                            | 30              | 463                                   | 476         | 324-628          |
| 289.5                 | 171.954                            | bulk organic matter    | Poz-5066  | 3460                            | 40              | 1993                                  | 1966        | 1825-2106        |
| 367.5                 | 228.389                            | bulk organic matter    | Poz-5067  | 3695                            | 35              | 2228                                  | 2232        | 2116-2347        |
| 403.5                 | 252.715                            | bulk organic matter    | GrA-32023 | <i>6535</i>                     | <i>40</i>       | <i>5068r</i>                          | <i>5790</i> | <i>5662-5919</i> |
| 495.5                 | 301.820                            | bulk organic matter    | GrA-32258 | 5065                            | 35              | 3598                                  | 3903        | 3729-4077        |
| 583.5                 | 336.751                            | bulk organic matter    | GrA-32086 | 5725                            | 40              | 4258                                  | 4794        | 4628-4959        |
| 729.5                 | 406.901                            | bulk organic matter    | GrA-32027 | 6420                            | 40              | 4953                                  | 5739        | 5589-5889        |
| 747.0                 | 415.219                            |                        |           |                                 |                 |                                       | 6096        | 5907-6185        |

blf: below lake floor; Corr.  $^{14}\text{C}$  Age: after subtraction of the estimated lake-carbon reservoir age of  $1467 \pm 44$   $^{14}\text{C}$  years (mean of three estimations; see Methods); SMM: Science Museum of Minnesota; Poz: Poznań Radiocarbon Laboratory; GrA: Rijksuniversiteit Groningen Radiocarbon Laboratory. Three outlying dates on bulk organic matter are indicated in italics.

**Table S2.** List of non-diatom phytoplankton taxa with diagnostic micro-remains recovered from Lake Yoa composite core OUNIK03/04.

***Chlorophyta***

Chlorococcales

Chlorococcaceae: *Tetraedron*

Dictyosphaeriaceae: *Botryococcus*

Hydrodictyaceae: *Pediastrum* (8 species), *Sorastrum*

Scenedesmaceae: *Coelastrum*, *Scenedesmus*

Desmidiiales

Desmidiaceae: *Cosmarium* (2 species), *Euastrum*, *Staurastrum*

Zygnematales

Zygnemataceae: *Spirogyra*

Colony-building coccoids

Oocystaceae: *Chlorella*

***Cyanobacteria***

Chroococcales

Chroococcaceae: *Chroococcus*, *Gloeotrichia*

***Dinophyta***

Dinophyceae: *Ceratium*

## Supplementary figures

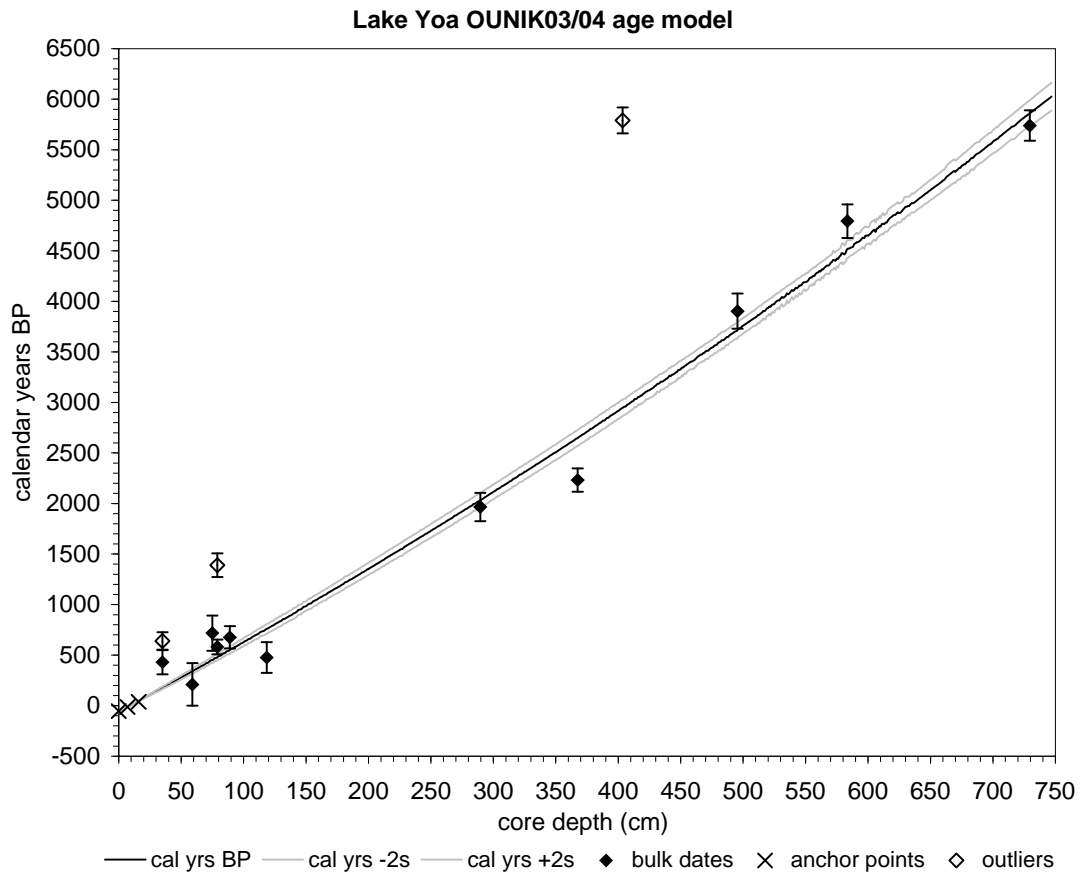


**Fig. S1.** Age-depth relationship of composite core OUNIK03/04 from Lake Yoa, based on a 3rd-order polynomial regression of 3 anchor points and 12 INTCAL04-calibrated  $^{14}\text{C}$  ages vs. cumulative dry weight down-core; see Methods section 2.

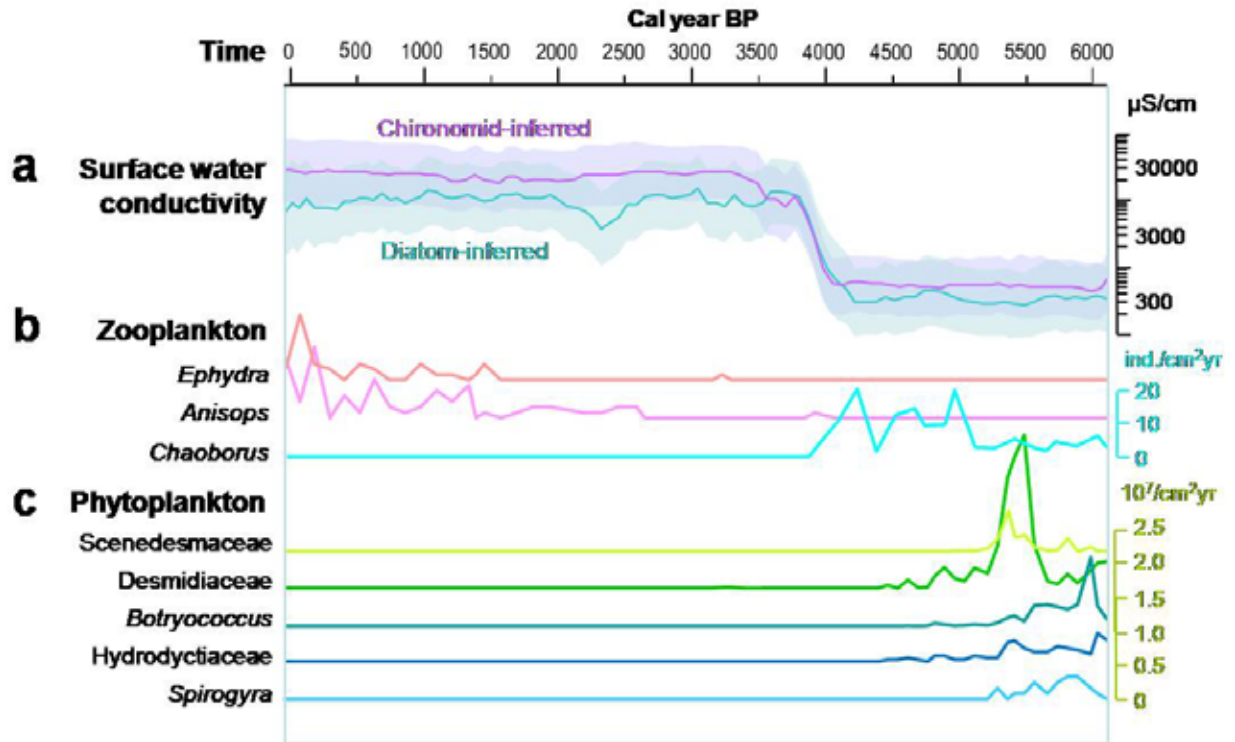


**Fig. S2.** Evolution of selected zooplankton and phytoplankton taxa in Lake Yoa over the past 6000 years.

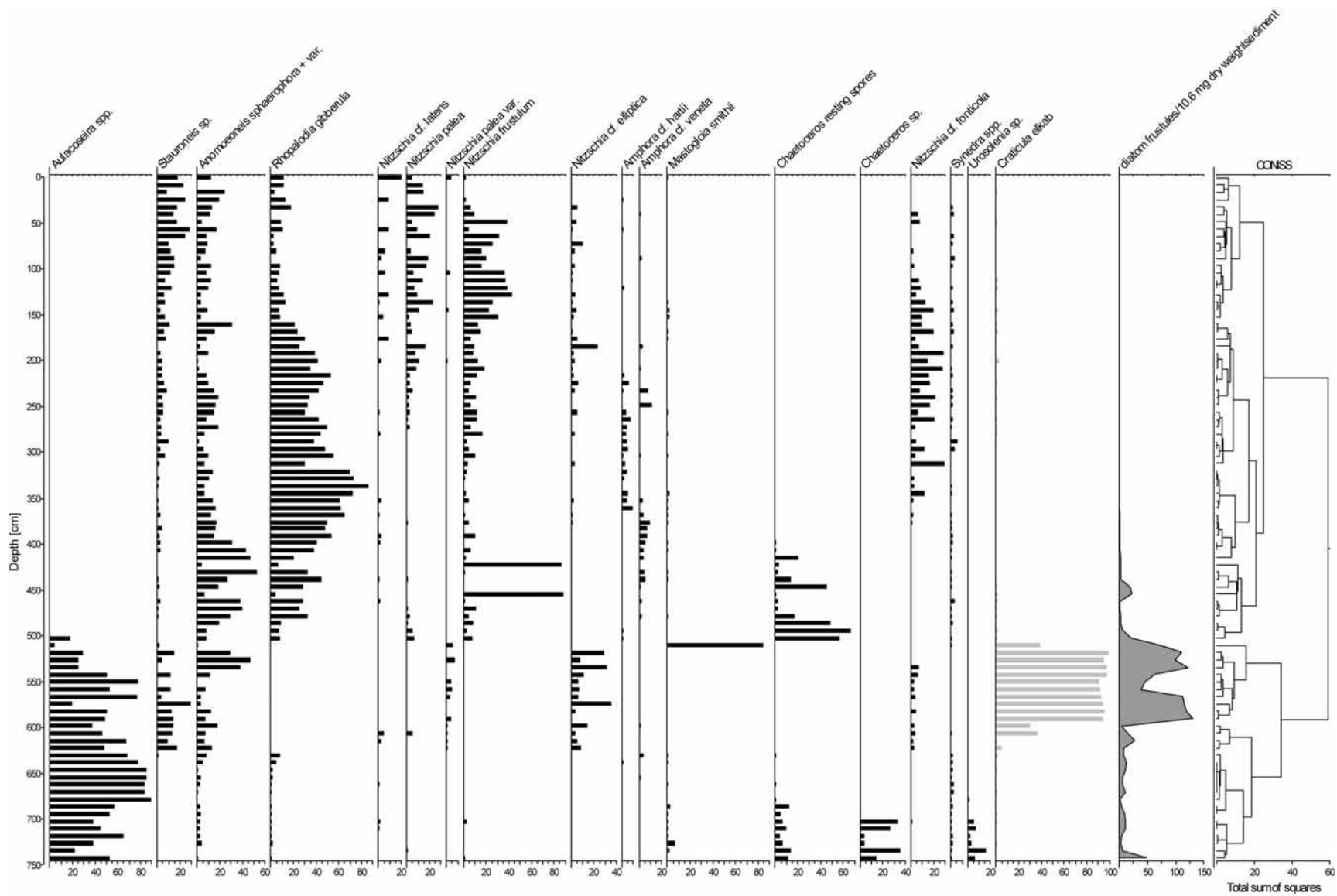


**Fig. S3.** Stratigraphic distribution of fossil diatom taxa [%] in composite core OUNIK03/04 from Lake Yoa, northern Chad. Biostratigraphic zonation is based on CONISS (Grimm 1987).

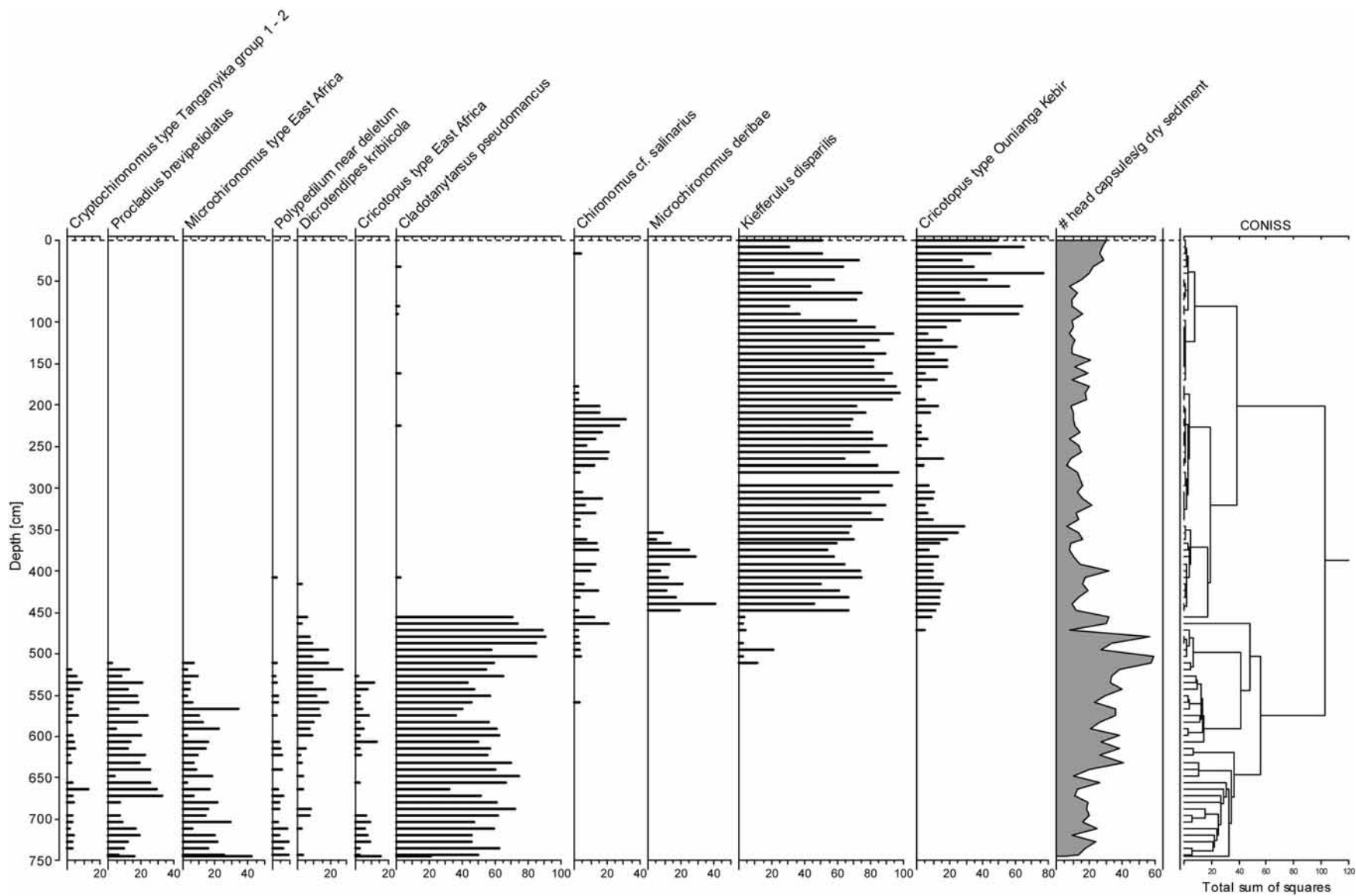


**Fig. S4.** Stratigraphic distribution of fossil chironomid taxa [%] in composite core OUNIK03/04 from Lake Yoa, northern Chad. Biostratigraphic zonation is based on CONISS (Grimm 1987).

## Supplementary references

- S1. S. Kröpelin, in *Atlas of Cultural and Environmental Change in Arid Africa*, O. Bubenzer, A. Bolten, F. Darius, Eds. (Heinrich-Barth-Institut, Köln, Germany, 2007), pp. 54-57.
- S2. H. E. Wright, *J. Sediment. Petrol.* **37**, 975 (1967).
- S3. P. G. Appleby, in *Tracking Environmental Change Using Lake Sediments: Basin Analysis, Coring, and Chronological Techniques*, W. M. Last, J. P. Smol, Eds. (Kluwer Academic Publishers, Dordrecht, The Netherlands, 2001), pp. 171-203.
- S4. P. J. Reimer *et al.*, *Radiocarbon* **46**, 1029 (2004).
- S5. H. J. Schrader, *Nova Hedwigia* **45**, 403 (1973).
- S6. C. Cocquyt, D. Schram, *Hydrobiologia* **436**, 59 (2000).
- S7. E. C. Grimm, *Comput. Geosci.* **13**, 13 (1987).
- S8. H. J. B. Birks, A. D. Gordon, Eds., *Numerical methods in Quaternary pollen analysis* (Academic Press, 1985) pp. 317.
- S9. K. D. Bennett, *New Phytol.* **132**, 155 (1996).
- S10. S. Juggins, *ZONE 1.2* (Environmental Change Research Center, University College London, London, 1991).
- S11. J. M. Line, H. J. B. Birks, unpublished software.
- S12. E. C. Grimm, *TILIA 2.0 version b.4* (Illinois State Museum, Research and Collection Center, Springfield, Illinois, 1993).
- S13. E. C. Grimm, *TGView version 2.0.2*. (Illinois State Museum, Research and Collection Center, Springfield, Illinois, 2004).
- S14. F. Gasse, S. Juggins, L. B. Khelifa, *Palaeogeogr. Palaeoclimatol. Palaeoecol.* **117**, 31 (1995).
- S15. A. L. Clarke *et al.*, *Limnol. Oceanogr.* **51**, 385 (2006).
- S16. H. J. B. Birks, in *Statistical Modelling of Quaternary Science Data*, D. Maddy, J. S. Brew, Eds. (Cambridge Quaternary Research Association, Cambridge, 1995), pp. 161-254.
- S17. S. Juggins, *C2, user Guide; Software for Ecological and Palaeoecological Data Analysis and Visualisation*. (University of Newcastle, Newcastle upon Tyne, United Kingdom, 1993).
- S18. I. R. Walker, in *Tracking Environmental Change using Lake sediments: Zoological Indicators*, J. Smol, H. J. B. Birks, W. Last, Eds. (Kluwer Academic Publishers, Dordrecht, The Netherlands, 2001), *Developments in Paleoenvironmental Research*, vol. 4, pp. 43-66.
- S19. D. Verschuren, H. Eggermont, *J. Paleolimnol.* **38**, 329 (2007).
- S20. D. Verschuren, *Arch. Hydrobiol. Beih.* **107**, 467 (1997).
- S21. H. Eggermont, D. Verschuren, *J. Paleolimnol.* **32**, 383 (2004a).
- S22. H. Eggermont, D. Verschuren, *J. Paleolimnol.* **32**, 413 (2004b).
- S23. H. Eggermont, D. Verschuren, H. J. Dumont, *J. Biogeogr.* **32**, 1063 (2005).
- S24. B. Rumes, H. Eggermont, D. Verschuren, *Hydrobiologia* **542**, 297 (2005).
- S25. O. Heiri, A. F. Lotter, *J. Paleolimnol.* **26**, 343 (2001).
- S26. R. Quinlan, J. P. Smol, *J. Paleolimnol.* **26**, 327 (2001).
- S27. H. Eggermont *et al.*, *Quat. Sci. Rev.* (submitted).
- S28. K. Faegri, J. Iversen. *Textbook of pollen analysis*. (Wiley, Chicester, 1989).
- S29. J. A. Dearing, in *Quaternary Climates, Environments and Magnetism*, B. A. Maher, R. Thompson, Eds. (Cambridge University Press, 1999) pp. 231-278.
- S30. B. A. Maher, R. Thompson (Eds.). *Quaternary climates, environments and magnetism*. (Cambridge University Press, 1999).

- S31. D. Nahon, *Palaeocol. Afr.* **12**, 63 (1980).
- S32. P. Hoelzmann *et al.*, in *Past climate variability through Europe and Africa*, R. W. Battarbee, F. Gasse, C. E. Stickley, Eds. (Kluwer, Dordrecht, Netherlands, 2004), pp. 219–256.
- S33. F. Gasse, *Quat. Sci. Rev.* **21**, 737 (2002).
- S34. D. Fleitmann *et al.*, *Science* **300**, 1737 (2003).
- S35. D. Verschuren, *Quat. Sci. Rev.* **18**, 821 (1999).
- S36. J. C. Ritchie, C. H. Eyles, C. V. Haynes, *Nature* **314**, 352 (1985).
- S37. A. M. Lézine, J. Casanova, C. Hillaire-Marcel, *Geology* **18**, 264 (1990).
- S38. J. Fabre & N. Petit-Maire, *Palaeogeogr. Palaeoclimatol. Palaeoecol.* **65**, 133 (1988).
- S39. Z. Liu *et al.*, *Quat. Sci. Rev.* **26**, 1818 (2007).
- S40. R. Kuper, S. Kröpelin, *Science* **313**, 803 (2006).
- S41. P. B. deMenocal *et al.*, *Quat. Sci. Rev.* **19**, 347 (2000).
- S42. J. Adkins, P. Demenocal, G. Eshel, *Paleoceanography* **21**, Art. No. PA4203 (2006).
- S43. J. B. Stuut *et al.*, *J. Geophys. Res.-Atmos.* **110**, Art. No. D04202 (2005).
- S44. R. Capot-Rey, *Mém. d'Institut de Recherches Sahariennes* **5** (1961).
- S45. D. Verschuren, J. Tibby, K. Sabbe, N. Roberts, *Ecology* **81**, 164 (2000).
- S46. D. S. Rawson, J. E. Moore, *Can. J. Res. D* **22**, 141 (1944).
- S47. U. T. Hammer, *Monogr. Biol.* **59** (1986), 616 pp.
- S48. S. Kröpelin, *Berliner Geogr. Abh.* **54** (1993).
- S49. M. Schuster *et al.*, *Quat. Sci. Rev.* **24**, 1821 (2005).
- S50. M. Thinon, A. Ballouche, M. Reille, *Holocene* **6**, 457 (1996).
- S51. F. Mees, D. Verschuren, R. Nijs, H. Dumont, *J. Paleolimnol.* **5**, 227 (1991).
- S52. M. Cremaschi, M. Pelfini, M. Santilli, *Holocene* **16**, 293 (2006).
- S53. N. Petit-Maire, Z. Guo, S. Kröpelin, *Global Planet. Change* **26**, 97 (2000).
- S54. H. Renssen, *Geophys. Res. Lett.* **30**, Art. No. 1184 (2003).
- S55. H. Renssen, V. Brovki, T. Fichet, H. Goosse, *Quatern. Int.* **150**, 95 (2006).
- S56. M. Sankaran *et al.*, *Nature* **438**, 846 (2005).
- S57. V. Brovkin, M. Claussen, V. Petoukhov, A. Ganopolski, *J. Geophys. Res.-Atm.* **103**, 31613 (1998).
- S58. S. Joussaume *et al.*, *Geophys. Res. Lett.* **26**, 859 (1999).
- S59. M. Scheffer, M. Holmgren, V. Brovkin, M. Claussen, *Global Change Biol.* **11**, 1003 (2005).
- S60. M. Baudena, G. Boni, L. Ferraris, J. von Hardenberg, A. Provenzale, *Adv. Water Resources* **30**, 1320 (2007).